Title	Extension of semi-analytical approach to determine natural frequencies and mode shapes of multi-span orthotropic bridge deck
Authors(s)	Rezaiguia, Abdelouahab, Fisli, Y., Ellagoune, S., et al.
Publication date	2012-07-10
Publication information	Rezaiguia, Abdelouahab, Y. Fisli, S. Ellagoune, and et al. “Extension of Semi-Analytical Approach to Determine Natural Frequencies and Mode Shapes of Multi-Span Orthotropic Bridge Deck” 43, no. 1 (July 10, 2012).
Publisher	Techno-press Ltd
Item record/more information	http://hdl.handle.net/10197/4874

Extension of a semi-analytical approach to determine natural frequencies and mode shapes of a multi-span orthotropic bridge deck

A. Rezaiguia[1a], Y. Fisli[1b], S. Ellagoune[1c], D.F. Laefer[*2d], N. Ouelaa[1,e]

[1]*Mechanics & Structures Laboratory, Guelma University, P.O.B 401, Guelma 24000, Algeria*

[2]*Urban Modeling Group, School of Architecture, Landscape, and Civil Engineering, University College, Belfield, Dublin 4, Ireland*

Abstract. This paper extends a single equation, semi-analytical approach for three-span bridges to multi-span ones for the rapid and precise determination of natural frequencies and natural mode shapes of an orthotropic, multi-span plate. This method can be used to study the dynamic interaction between bridges and vehicles. It is based on the modal superposition method taking into account intermodal coupling to determine natural frequencies and mode shapes of a bridge deck. In this paper, a four- and a five-span orthotropic roadway bridge decks are compared in the first 10 modes with a finite element method analysis using ANSYS software. This simplified implementation matches numerical modeling within 2% in all cases. The paper verifies that applicability of single formula approach as a simpler alternative to finite element modeling.

Keywords: natural frequencies; natural mode shapes; multi-span orthotropic bridge deck; dynamic loading; traffic.

---

[*]Corresponding author, Tenured Lecturer, debra.laefer@ucd.ie
[a] Research Professor, Dr., a.rezaiguia@gmail.com
[b] Research Scholar, Master
[c] Research Professor, Dr.
[d] Research Professor, Dr.

1. Introduction

Dynamic analysis of a bridge commences with the determination of the natural frequencies and natural mode shapes of vibration of the decks, especially when the modal method is used. Most

bridge decks are orthotropic, because of the orthotropic nature of their component parts (e.g. isotropic slabs, grillages, T-beam bridge decks, multi-beam bridge decks, multicell box-beam bridge, and slabs stiffened with ribs of box section). Thus, the orthotropic plate theory plays an important role in the static and dynamic analysis of bridges. For example, a multicellular Fiber Reinforced Polymer (FRP) composite bridge deck can be modeled as an orthotropic plate (Davalos et al. 2006) with equivalent stiffnesses that account for the size, shape, and constituent materials of the cellular deck. Thus, the complexity of material anisotropy of the panels and orthotropic structure of the deck system can be reduced to an equivalent orthotropic plate with global elastic properties in two orthogonal directions – parallel and transverse to the longitudinal axis of the deck cell.

To date, there have been three main methods approaches to dynamic analysis of bridge decks: (1) finite element, (2) finite strip, and (3) orthotropic plate theory methods. The last is applicable to vibration analysis bridge decks that are slabs, composite, orthotropic, right, curved and simply supported. Several analytical, semi-analytical and numerical methods have been developed previously to determine natural frequencies and natural modes shapes of multi-span continuous plates. For example, the state-space-based differential quadrature method proposed by Bellman and Casti (1971) was used by Gorman and Garibaldi (2006) to obtain an accurate analytical solution for free vibration of a three-span bridge deck modeled as an isotropic rectangular plate having internal rigid line supports with different boundary conditions. The same method was used also by Lu et al. (2007) for a free vibration analysis of a continuous isotropic plate in one direction with mixed boundary conditions. The Levy-type series solution and the superposition method were used by Ng and Kaul (1987) to solve a continuous orthotropic plate problem with bridge-type boundary conditions, while Zhu and Law (2002) investigated the dynamic behavior of a continuous, multi-lane, bridge deck under a passing vehicle with seven degrees of freedom. In that case, the bridge deck was modeled as a multi-span, continuous, orthotropic, rectangular plate with rigid intermediate supports. The eigenfunctions of those bridges three spans in one direction and the single span beam

in the other direction were used as inputs for the Rayleigh-Ritz method to determine the natural frequencies of the plate. Zhou and Cheung (1999) used the same static beam functions in the Rayleigh-Ritz method to determine the natural frequencies and mode shapes of thin, orthotropic, rectangular, continuous plates in one and two directions. They showed that this set of static beam functions has advantages in terms of computational cost, application versatility, and numerical accuracy, especially for the plate problem with a large number of intermediate lines supported and/or when higher vibrating modes need to be calculated. Cheung et al. (1971) used the finite-strip method, while Wu and Cheung (1974) devised a method of finite elements in conjunction with Bolotin's method to analyze continuous plates in two directions. The finite element method approach has been widely adopted for analysis of plates with complex geometries (Zhou and Cheung, 1999; Hrabok and Hrudley, 1984; Smith and William, 1970). Recently Rezaiguia and Laefer (2009) introduced the concept of intermodal coupling for a three-span bridge deck, as will be described below.

The research presented herein was undertaken to understand the extent of the applicability of the intermodal coupling approach for more complicated bridges than previously established. As such, it was applied to a series of four-, and five-span bridge decks. The value of such work is in ascertaining whether a high precision solution for natural frequency determination can be obtained using only a single equation, instead of the thousands that must be solved using current finite element approaches (e.g. as implemented in ANSYS). The work is highly relevant with respect to evaluating the dynamic interaction between bridges and vehicles.

2. Natural frequencies and mode shapes of a multi-span orthotropic bridge deck

The bridge deck (fig. 1) was modeled as a multi-span, continuous, orthotropic, rectangular, thin plate with an arbitrary number of line-rigid, intermediate supports (fig. 2). Using the modal superposition method, the free harmonic vibration of a thin orthotropic plate with a constant thickness h is governed by the differential eq.(1)

$$D_x \frac{\partial^4 \phi_{ij}}{\partial x^4} + 2H \frac{\partial^4 \phi_{ij}}{\partial x^2 \partial y^2} + D_y \frac{\partial^4 \phi_{ij}}{\partial y^4} - \omega_{ij}^2 \rho h \phi_{ij} = 0 \tag{1}$$

where $\phi_{ij}(x,y)$ are the mode shapes of a multi-span continuous orthotropic plate. The quantities $D_x=E_x h^3/12(1-\nu_{xy}\nu_{yx})$, $D_y=D_x E_y/E_x$, $H=\nu_{xy}D_y+2D_{xy}$ and $D_{xy}=G_{xy}h^3/12$ are flexural rigidities with E_x and E_y are Young's moduli, ν_{xy} and ν_{yx} are Poisson's ratios and G_{xy} is the shear modulus. ω_{ij} are the natural frequencies of a multi-span orthotropic plate, and ρ is the mass density. Eq.(1) also applies to the isotropic case, for which $\nu_{xy}=\nu_{yx}=\nu$, $D_x=D_y=H=Eh^3/12(1-\nu^2)$ and $D_{xy}=D(1-\nu)/2$.

Although several authors have expressed $\phi_{ij}(x,y)$ as the product of two admissible functions $\varphi_i(x)$ and $h_j(y)$, which are eigenfunctions of beams, this decomposition neglects the intermodal coupling between longitudinal and transversal modes, which can affect natural frequencies. To take into account the intermodal coupling, the solution adopted herein is that proposed by Rezaiguia and Laefer (2009) where $\phi_{ij}(x,y)$ is expressed as the product of two admissible functions: $\varphi_i(x)$ are eigenfunctions of multi-span continuous beam, and $h_{ij}(y)$ are eigenfunctions of single span beam satisfying the boundary conditions of plate. This decomposition may be expressed as eq. (2)

$$\phi_{ij}(x,y) = \varphi_i(x) h_{ij}(y) \tag{2}$$

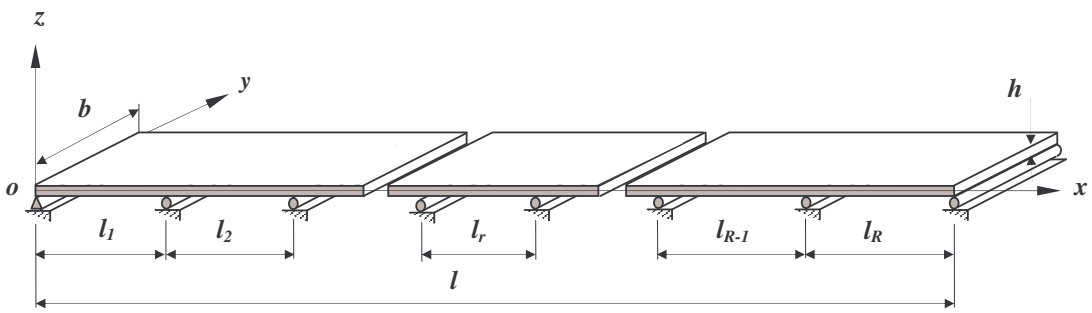

Fig. 1. Model of the continuous multi-span bridge deck

2.1. Eigenvalues k_i and eigenfunctions $\varphi_i(x)$ of multi-span continuous beam

To determine the eigenvalue and eigenfunctions of a multi-span continuous beam (fig. 2), it is necessary to determine the eigenfunctions for each span. The expression of *i*th mode shape for the transverse vibration in the *r*th span is as reflected in eq. (3):

$$\varphi_{ri}(x_r) = A_{ri}\sin(k_i x_r) + B_{ri}\cos(k_i x_r) + C_{ri}\sinh(k_i x_r) + D_{ri}\cosh(k_i x_r), \quad r = 1, 2, ..., R \tag{3}$$

where A_{ri}, B_{ri}, C_{ri}, and D_{ri} are determined by the application of the boundary conditions and the continuity conditions at the intermediate supports; k_i is the eigenvalue of the *i*th eigenfunction of multi-span beam vibration; and R is the number of spans.

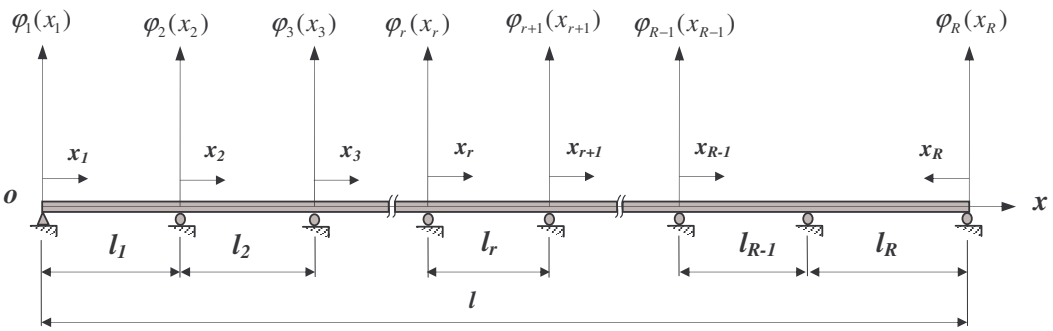

Fig. 2. Continuous multi-span simply supported beam

Zhu and Law (2001) presented the formulation of the eigenfunctions and mode shapes of a multi-span continuous beam. However, there are simplifications in their expressions and indices, which introduce errors. The boundary and continuity conditions are as listed as follows:

The vertical deflection is equal to zero at all supports:

$$\varphi_r(x_r)\big|_{x_r=0} = \varphi_r(x_r)\big|_{x_r=l_r} = 0, \quad r = 1, 2, ..., R \tag{4.1}$$

The bending moments are equal to zero at the ends:

$$\left.\frac{d^2\varphi_1(x_1)}{dx_1^2}\right|_{x_1=0} = \left.\frac{d^2\varphi_R(x_R)}{dx_R^2}\right|_{x_R=0} = 0 \tag{4.2}$$

The slope and bending moments at the intermediate supports are continuity conditions:

$$\left.\frac{d\varphi_r(x_r)}{dx_r}\right|_{x_r=l_r} = \left.\frac{d\varphi_{r+1}(x_{r+1})}{dx_{r+1}}\right|_{x_{r+1}=0} \qquad r = 1,\ 2,\ ...,\ R-2 \tag{4.3}$$

$$\left.\frac{d^2\varphi_r(x_r)}{dx_r^2}\right|_{x_r=l_r} = \left.\frac{d^2\varphi_{r+1}(x_{r+1})}{dx_{r+1}^2}\right|_{x_{r+1}=0} \qquad r = 1,\ 2,\ ...,\ R-2 \tag{4.4}$$

$$\left.\frac{d\varphi_{R-1}(x_{R-1})}{dx_{R-1}}\right|_{x_{R-1}=l_{R-1}} = -\left.\frac{d\varphi_R(x_R)}{dx_R}\right|_{x_R=l_R} \tag{4.5}$$

$$\left.\frac{d^2\varphi_{R-1}(x_{R-1})}{dx_{R-1}^2}\right|_{x_{R-1}=l_{R-1}} = \left.\frac{d^2\varphi_R(x_R)}{dx_R^2}\right|_{x_R=l_R} \tag{4.6}$$

Substituting all the boundary and continuity conditions (4.1) to (4.6) into expression (3), after many manipulations and simplifications, one obtains eigenfunctions of multi-span continuous beam:

For $0 \le x \le l_1$:

$$\varphi_i(x) = A_{1i}\left(\sin(k_i x) - \frac{\sin(k_i l_1)}{\sinh(k_i l_1)}\sinh(k_i x)\right) \tag{5.1}$$

For $\sum_{j=1}^{r-1} l_j \le x \le \sum_{j=1}^{r} l_j$:

$$\varphi_i(x) = A_{ri}\left(\sin\left(k_i\left(x-\sum_{j=1}^{r-1} l_j\right)\right) - \frac{\sin(k_i l_r)}{\sinh(k_i l_r)}\sinh\left(k_i\left(x-\sum_{j=1}^{r-1} l_j\right)\right)\right) + B_{ri}\left(\cos\left(k_i\left(x-\sum_{j=1}^{r-1} l_j\right)\right)\right.$$
$$\left.-\cosh\left(k_i\left(x-\sum_{j=1}^{r-1} l_j\right)\right) + \frac{\cosh(k_i l_r)-\cos(k_i l_r)}{\sinh(k_i l_r)}\sinh\left(k_i\left(x-\sum_{j=1}^{r-1} l_j\right)\right)\right),$$

$$r = 2, 3, ..., R-1 \text{ and } R \ge 3 \tag{5.2}$$

For $l - l_R \le x \le l$:

$$\varphi_i(x) = A_{Ri}\left(\sin(k_i(l-x)) - \frac{\sin(k_i l_R)}{\sinh(k_i l_R)}\sinh(k_i(l-x))\right) \tag{5.3}$$

where k_i, A_{1i}, A_{ri}, B_{ri}, $r = 2, 3, ..., R-1$ and A_{Ri} are determined by solving eq. (6):

$$[F]\{A\} = \{0\} \tag{6}$$

The elements in vector $\{A\}$ and matrix $[F]$ are given in Appendix A, also for both the four-span and five-span cases. For a non-trivial solution, the determinant of the matrix $[F]$ must be zero, which gives the frequency equation. The solution of this equation yields eigenvalues k_i generated within the software Mathematica v.4. For each value of k_i, the resolution of the algebraic linear system of eqs. (6) is obtained by the Gauss method.

2.2. Determination of natural frequencies ω_{ij} and eigenfunctions $h_{ij}(y)$

To take account of the intermodal coupling, mode shapes in the y-direction are presented as the function $h_{ij}(y)$, thus satisfying the boundary conditions of a plate at the free edges $y = 0$ and $y = b$. Determination of $h_{ij}(y)$ function is presented in detail in reference Rezaiguia and Laefer (2009). To clarify this paper for the reader, it is necessary to include a summary of the approach in which the function $h_{ij}(y)$ is obtained.

The differential eq. (1) must be satisfied for all values of x, but determining its resolution for every value of x is practically impossible to achieve. For this reason, it is proposed to substitute expression (2) into eq. (1) and then multiply it by $\varphi_i(x)$ and integrating over the bridge length. From this, one obtains eq. (7):

$$D_y \frac{d^4 h_{ij}}{dy^4} \int_0^l \varphi_i^2 dx + 2H \frac{d^2 h_{ij}}{dy^2} \int_0^l \varphi_i'' \varphi_i dx + \left(D_x k_i^4 - \rho h \omega_{ij}^2\right) h_{ij} \int_0^l \varphi_i^2 dx = 0 \tag{7}$$

Dividing eq. (7) by $D_y \int_0^l \varphi_i^2 dx$, one obtains:

$$\frac{d^4 h_{ij}}{dy^4} + \frac{2Hk_{1i}^2}{D_y} \frac{d^2 h_{ij}}{dy^2} + \left(\left(D_x k_i^4 - \rho h \omega_{ij}^2\right) / D_y\right) h_{ij} = 0 \tag{8}$$

With a new frequency parameter

$$k_{1i} = \sqrt{\int_0^l \varphi_i'' \varphi_i dx / \int_0^l \varphi_i^2 dx} \tag{9}$$

Hence, the solution of eq. (8) is given by the general form in eq. (10):

$$h_{ij}(y) = A_{ij} e^{s_{ij} y} \tag{10}$$

Substituting expression (10) into eq. (8), one obtains eq. (11):

$$s_{ij}{}^4 - \frac{2Hk_{1i}^2}{D_y} s_{ij}{}^2 + \left(D_x k_i^4 - \rho h \omega_{ij}^2\right) / D_y = 0 \tag{11}$$

The roots of the eq. (11) are eqs. (12a) and (12b):

$$s_{1ij} = \pm \frac{1}{\sqrt{D_y}} \sqrt{Hk_{1i}^2 + \sqrt{H^2 k_{1i}^4 - D_y \left(D_x k_i^4 - \rho h \omega_{ij}^2\right)}} = \pm r_{1ij} \tag{12a}$$

$$s_{2ij} = \pm J \frac{1}{\sqrt{D_y}} \sqrt{Hk_{1i}^2 - \sqrt{H^2 k_{1i}^4 - D_y \left(D_x k_i^4 - \rho h \omega_{ij}^2\right)}} = \pm J r_{2ij} \tag{12b}$$

Note that the parameters r_{1ij} and r_{2ij} are not independent but are related by the pulsations ω_{ij}. Substituting solutions (12a and 12b) into expression (10), and replacing exponential functions by trigonometric and hyperbolic functions, one obtains eq. (13):

$$h_{ij}(y) = C_{ij} \sin(r_{2ij} y) + D_{ij} \cos(r_{2ij} y) + E_{ij} \sinh(r_{1ij} y) + F_{ij} \cosh(r_{1ij} y) \tag{13}$$

where C_{ij}, D_{ij}, E_{ij} and F_{ij} are new constants of integration. They are determined by the application of the boundary conditions at the free edges of the bridge deck: $y = 0$ and $y = b$. At these edges, the bending moment and the shear force are zero. Taking account of the expressions (2), these boundary conditions become (Rezaiguia and Laefer, 2009):

$$\begin{aligned}
&D_y \frac{d^2 h_{ij}}{dy^2}(0) - \nu_{yx} D_x k_{1i}^2 h_{ij}(0) = 0 \\
&D_y \frac{d^3 h_{ij}}{dy^3}(0) - \left(\nu_{yx} D_x + 4D_{xy}\right) k_{1i}^2 \frac{dh_{ij}}{dy}(0) = 0 \\
&D_y \frac{d^2 h_{ij}}{dy^2}(b) - \nu_{yx} D_x k_{1i}^2 h_{ij}(b) = 0 \\
&D_y \frac{d^3 h_{ij}}{dy^3}(b) - \left(\nu_{yx} D_x + 4D_{xy}\right) k_{1i}^2 \frac{dh_{ij}}{dy}(b) = 0
\end{aligned} \tag{14}$$

The application of the boundary conditions from eq (14) in eq. (13), gives the following system as shown in eq. (15):

$$\begin{bmatrix} 0 & \alpha_{ij} & 0 & \theta_{ij} \\ \gamma_{ij} & 0 & \chi_{ij} & 0 \\ \alpha_{ij}\sin(r_{2ij}b) & \alpha_{ij}\cos(r_{2ij}b) & \theta_{ij}\,sh(r_{1ij}b) & \theta_{ij}\,ch(r_{1ij}b) \\ \gamma_{ij}\cos(r_{2ij}b) & -\gamma_{ij}\sin(r_{2ij}b) & \chi_{ij}\,ch(r_{1ij}b) & \chi_{ij}\,sh(r_{1ij}b) \end{bmatrix} \begin{Bmatrix} C_{ij} \\ D_{ij} \\ E_{ij} \\ F_{ij} \end{Bmatrix} = \begin{Bmatrix} 0 \\ 0 \\ 0 \\ 0 \end{Bmatrix} \tag{15}$$

with

$$\alpha_{ij} = -D_y r_{2ij}^2 - \nu_{yx} D_x k_{1i}^2 \tag{16.a}$$

$$\theta_{ij} = D_y r_{1ij}^2 - \nu_{yx} D_x k_{1i}^2 \tag{16.b}$$

$$\gamma_{ij} = -D_y r_{2ij}^3 - (\nu_{yx} D_x + 4D_{xy})\, r_{2ij} k_{1i}^2 \tag{16.c}$$

$$\chi_{ij} = D_y r_{1ij}^3 - (\nu_{yx} D_x + 4D_{xy})\, r_{1ij} k_{1i}^2 \tag{16.d}$$

For non-trivial solutions of the system (15), the frequency equation is eq. (17)

$$2\alpha_{ij}\theta_{ij}\gamma_{ij}\chi_{ij}\,(-1+\cos(r_{2ij}b)\cosh(r_{1ij}b)) + (\theta_{ij}^2\gamma_{ij}^2 - \alpha_{ij}^2\chi_{ij}^2)\sin(r_{2ij}b)\sinh(r_{1ij}b) = 0 \tag{17}$$

The parameters r_{1ij} or r_{2ij} can be solved from eq. (17), while the natural frequency ω_{ij} can be obtained from expressions (12a) and (12b).

To determine expressions of the new constants of integration, one simplifies the system (15) by normalization of the first component C_{ij} of the unknown vector with 1, thereby reducing the problem to 4 equations with 3 unknown, from which one obtains the expressions for the constants D_{ij}, E_{ij}, and F_{ij} :

$$D_{ij} = (\alpha_{ij}\sin(r_{2ij}b) - \frac{\gamma_{ij}\theta_{ij}}{\chi_{ij}}\sinh(r_{1ij}b)) / \alpha_{ij}(\cosh(r_{1ij}b) - \cos(r_{2ij}b)) \tag{18.a}$$

$$E_{ij} = -\gamma_{ij} / \chi_{ij} \tag{18.b}$$

$$F_{ij} = (-\alpha_{ij}\sin(r_{2ij}b) + \frac{\gamma_{ij}\theta_{ij}}{\chi_{ij}}\sinh(r_{1ij}b)) / (\theta_{ij}\cosh(r_{1ij}b) - \theta_{ij}\cos(r_{2ij}b)) \tag{18.c}$$

To calculate the natural frequencies ω_{ij} of the multi-span orthotropic bridge deck, first k_i values were calculated. Second the k_{1i} values were determined using expression (9). Subsequently,

Mathematica software was used to determine the roots r_{1ij} or r_{2ij} of the frequency eq. (17). Finally, natural frequencies of the multi- span bridge deck ω_{ij} were calculated by expressions (12a) and (12b).

3. Numerical examples

To validate the generalization of the method presented in this paper, two examples are prepared:

- a continuous orthotropic four-span multi-girder bridge deck (fig.3a) with length l = 108 m and span lengths $l_1 = l_4$ = 24 m and $l_2 = l_3$ = 30 m. The parameters of the bridge deck are listed in table 1.
- a continuous orthotropic five-span multi-girder bridge deck (fig.3b) with length l = 138 m and span lengths $l_1 = l_5$ = 24 m and $l_2 = l_3 = l_4$ = 30 m. The parameters of the bridge deck are listed in table 2.

Table 1. Parametres of four span multi-girder bridge deck

Concrete Deck slab:	
Length	108 m
Width	13.715 m
Thickness	0.2 m
Young's moduli	$E_x = 4.17\times10^{10}$ N/m^2, $E_y = 2.97\times10^{10}$ N/m^2
Mass density	3000 kg/ m^3
Poisson's ratio	$\nu_{xy} = 0.3$
Steel girders:	
Number	5
Distance between to adjacent girders	2.743 m
Web height	1.49 m
Web thickness	0.0111 m
Flange width	0.405 m
Flange thickness	0.018 m
Mass density	7850 kg/ m^3
Steel diaphragms:	
Number	19
Distance between to adjacent diaphragms	6 m
Cross-sectional area	15.48×10^{-4} m^2
Mass density	7850 kg/ m^3
Moments of inertia	$I_y = 0.71\times10^{-6}$ m^4, $I_z = 2\times10^{-6}$ m^4, $J = 1.2\times10^{-7}$m^4

In the reference case used herein published by Zhu and Law (2002), the equivalent orthotropic plate data were not explicitly provided. Instead, equivalent rigidities D_x, D_y and D_{xy} were published. From those, Rezaiguia (2008) made a homogenization of this composite structure to explore the concept of the volumic and massic fractions of a reinforced composite material. This homogenization takes into account all properties of this composite structure (deck slab, girders and diaphragms). From those all the equivalent orthotropic plate properties were obtained by conserving equivalent rigidities D_x, D_y and D_{xy}.The other following features of the equivalent orthotropic bridge decks were as follows: b = 13.715 m, h = 0.212 m, ρ = 3265 kg m^{-3}, $D_x = 2.41 \times 10^9$ N m, $D_y = 2.18 \times 10^7$ N m, $D_{xy} = 1.14 \times 10^8$ N m, $\nu_{xy} = 0.3$, $E_x = 3.06\times10^{12}$ N m^{-2}, $E_y = 2.76 \times 10^{10}$ N m^{-2}, $G_{xy} = 1.45 \times 10^{11}$ N m^{-2}. These were the same characteristics that were previously used to validate a three-span bridge with independent, external confirmation (Zhu and Law, 2002; Rezaiguia, 2008).

Table 2. Parametres of five span multi-girder bridge deck

Concrete Deck slab:	
Length	138 m
Width	13.715 m
Thickness	0.2 m
Young's moduli	$E_x = 4.17\times10^{10}$ N/m^2, $E_y = 2.97\times10^{10}$ N/m^2
Mass density	3000 kg/ m^3
Poisson's ratio	$\nu_{xy} = 0.3$
Steel girders:	
Number	5
Distance between to adjacent girders	2.743 m
Web height	1.49 m
Web thickness	0.0111 m
Flange width	0.405 m
Flange thickness	0.018 m
Mass density	7850 kg/ m^3
Steel diaphragms:	
Number	24
Distance between to adjacent diaphragms	6 m
Cross-sectional area	15.48×10^{-4} m^2
Mass density	7850 kg/ m^3
Moments of inertia	$I_y = 0.71\times10^{-6}$ m^4, $I_z = 2\times10^{-6}$ m^4, $J = 1.2\times10^{-7}$m^4

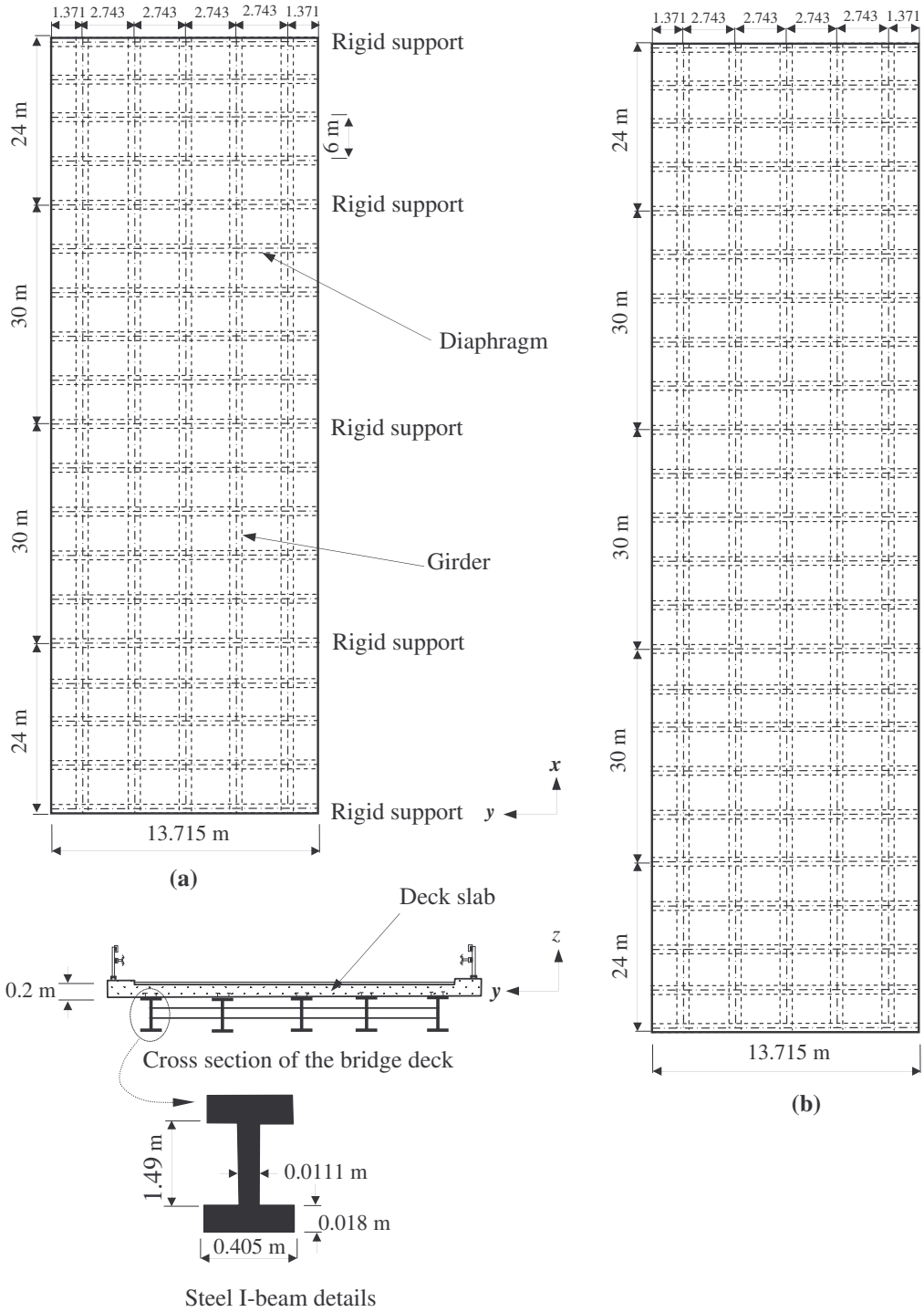

Fig. 3. Continuous multi-span multi-girder bridge deck: (a) four span, (b) five span

The finite element comparison was done in ANSYS v10. To calculate the ANSYS results, firstly all material properties of equivalent orthotropic plate for each case reported herein were numerically modelled. The element type used to mesh the bridge deck was shell 63 with 4 nodes and 6 degrees-of-freedom per node. The modal analysis type and block LANCZOS extraction method were used. The Finite Element Method (FEM) approach adopted herein had been previously verified (Rezaiguia and Laefer, 2009) against the three-span bridge work by Zhu and Law (2002). The FEM results of that study were within 2%. The convergence according of the mesh density for each case in the study presented herein is summarised in Table 3.

Table 3. Mesh density convergence

	Four-span			Five-span		
Mode	108×10	216×20	432×40	138×10	276×20	552×40
1	3.7745	3.7737	3.7736	3.5986	3.5995	3.5997
2	5.0981	5.0911	5.0891	4.4983	4.5002	4.5007
3	5.0985	5.0980	5.0978	4.9241	4.9225	4.9220
4	6.3376	6.3310	6.3290	5.7421	5.7429	5.7430
5	6.8441	6.8442	6.8442	5.7503	5.7541	5.7550
6	7.6647	7.6680	7.6687	6.9061	6.9112	6.9124
7	8.0449	8.0378	8.0354	7.1041	7.1106	7.1121
8	8.6712	8.6700	8.6446	7.6079	7.6169	7.6190
9	8.8158	8.6810	8.6693	8.2287	8.2387	8.2410
10	9.9226	9.7868	9.7494	8.5846	8.5100	8.4846

Table 4 presents the differences between the values of the first ten natural frequencies for two cases of the bridge deck. The analysis and comparison of results shows excellent agreement for all frequencies (errors not exceeding 2%), which confirms the validity of the generalisation of the proposed method for calculating the frequencies and mode shapes of multi-span orthotropic bridge deck. However, there is a slight difference between certain frequencies of tensional modes. This is mainly due to the influence of the side effects (shear deformation and rotary inertia), neglected in this approach. Fig. 4 shows the first four mode shapes of the four-span bridge deck obtained by the proposed approach (using FORTRAN language with the results plotted in MATLAB). Those

obtained from the FEM work in ANSYS are shown in fig. 5. Similarly, figs. 6 and 7 depict the five-span bridge deck. Excellent agreement between the mode shapes is seen.

Table 4. Comparison of natural frequencies of the orthotropic multi-span bridge decks

	Four-span			Five-span		
Mode	Present approach	ANSYS	Error (%)	Present approach	ANSYS	Error (%)
1	3.7724	3.7736	- 0.0318	3.5936	3.5997	- 0.1697
2	5.0905	5.0891	0.0275	4.4942	4.5007	- 0.1446
3	5.0927	5.0978	- 0.1001	4.9186	4.9220	- 0.0691
4	6.4501	6.3290	1.8774	5.7455	5.7430	0.0435
5	6.8385	6.8442	- 0.0833	5.7489	5.7550	- 0.1061
6	7.6651	7.6687	- 0.0469	6.9295	6.9124	0.2467
7	8.0311	8.0354	- 0.0535	7.1118	7.1121	- 0.0042
8	8.6612	8.6446	0.1916	7.6174	7.6190	- 0.0210
9	8.6813	8.6693	0.1382	8.2410	8.2410	0.0000
10	9.7719	9.7494	0.2302	8.5927	8.4846	1.2580

To better understand the potential advantages of using the Rezaiguia and Laefer (2009) approach, a more rigorous comparative discussion is needed. While Zhu and Law (2002) used the Rayleigh-Ritz method based on the Hamiltonian principle (minimization of a functional). The vertical displacement for free vibration of the plate is expressed by modal superposition method, where the mode shapes of the plate are decomposed as a series of functions. Specifically by employing polynomial beam functions along the x and y directions along with modal amplitudes, the Hamiltonian principle can be employed by taking the Rayleigh-Ritz derivation with respect to each coefficient to generate the eigenvalue equation in matrix form. Numerical resolution of that system yields natural frequencies and modal amplitudes and derivable mode shapes. While this semi-analytical method gives good results, its implementation is very complicated. A hundred integrals are needed to calculate mass and rigidity matrix as explicitly compared by Rezaiguia (2008) for a single-span bridge. Furthermore, the decomposition of mode shapes does not take account the intermodal coupling that affects the combined flexion-torsion natural frequencies and

mode shapes. It is known that free-free beam eigenfunctions (y direction), do not satisfy exactly the free edge beam boundary conditions (Gorman and Garibaldi, 2006). This is because of the mixed derivatives that appear in the formulation of plate free edge conditions.

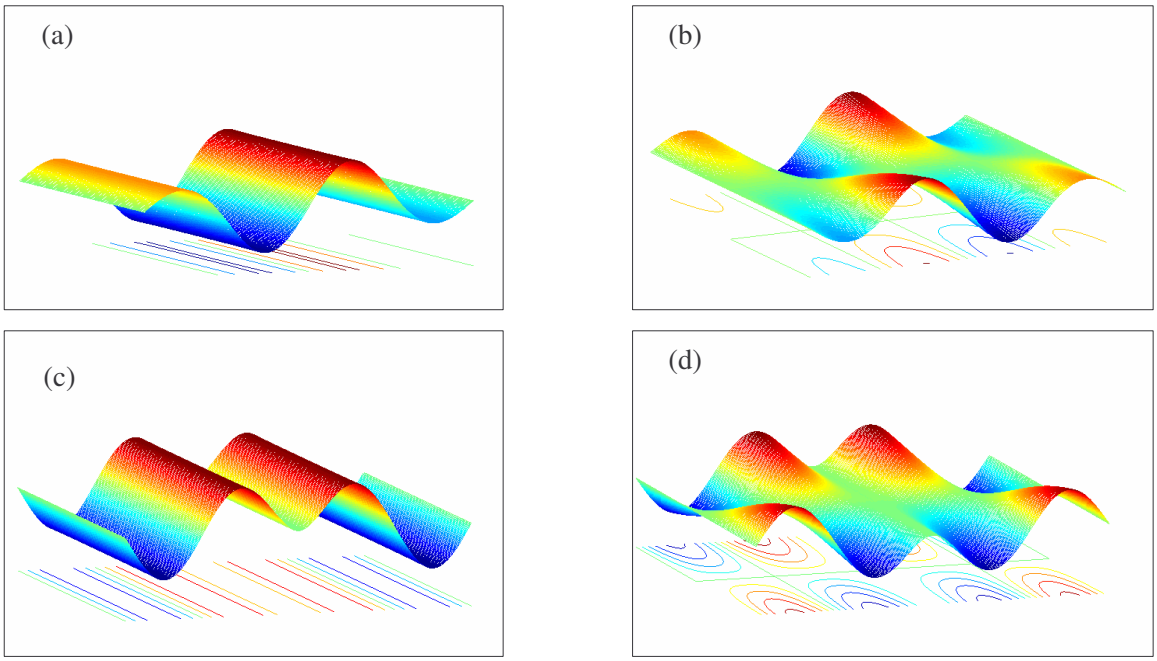

Fig. 4. The first four mode shapes of the four-span bridge deck obtained through the present approach. Modes: (a) 1, f_1 = 3.7724 Hz; (b) 2, f_2 = 5.0905; (c) 3, f_3 = 5.0927 Hz; (d) 4, f_4 = 6.4501 Hz

While the Rezaiguia and Laefer (2009) approach is also semi- analytical and similarly employs modal superposition to express the vertical displacement for free vibration of the plate by modal superposition method, the calculation of the natural frequencies and natural mode shapes of the bridge deck is handled differently. The derivation of the eigenvalue equation in the two methods is completely different as is the decomposition of mode shapes. Specifically, Zhu and Law's decomposition (Zhu and Law, 2001; 2002) does not take into account the intermodal coupling, which affects natural frequencies for the combined flexion-torsion modes. The Rezaiguia and Laefer (2009) approach incorporates the intermodal coupling, because the $h_{ij}(y)$ function satisfies the boundary conditions of a plate at the free edges of the bridge deck. Furthermore it allows expressions of the polynomial beam functions along x and y directions, respectively, that are not

explicit in Zhu and Law's approach. All of this has been achieved while also avoiding the cumbersome mathematical calculation of hundreds integrals needed to calculate the mass and rigidity matrix in Rayleigh-Ritz method.

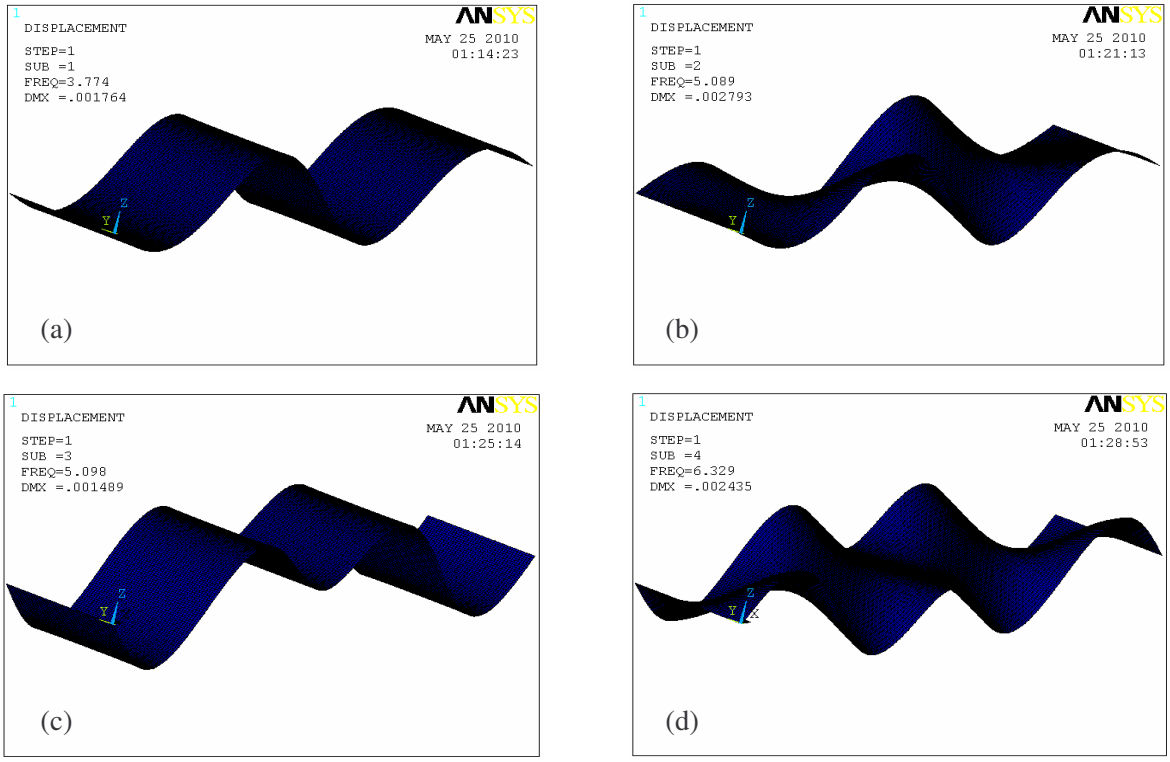

Fig. 5. The first four mode shapes of the four-span bridge deck obtained through ANSYS. Modes: (a) 1, f_1 = 3.7736 Hz; (b) 2, f_2 = 5.0891 Hz; (c) 3, f_3 = 5.0978 Hz; (d) 4, f_4 = 6.3290 Hz

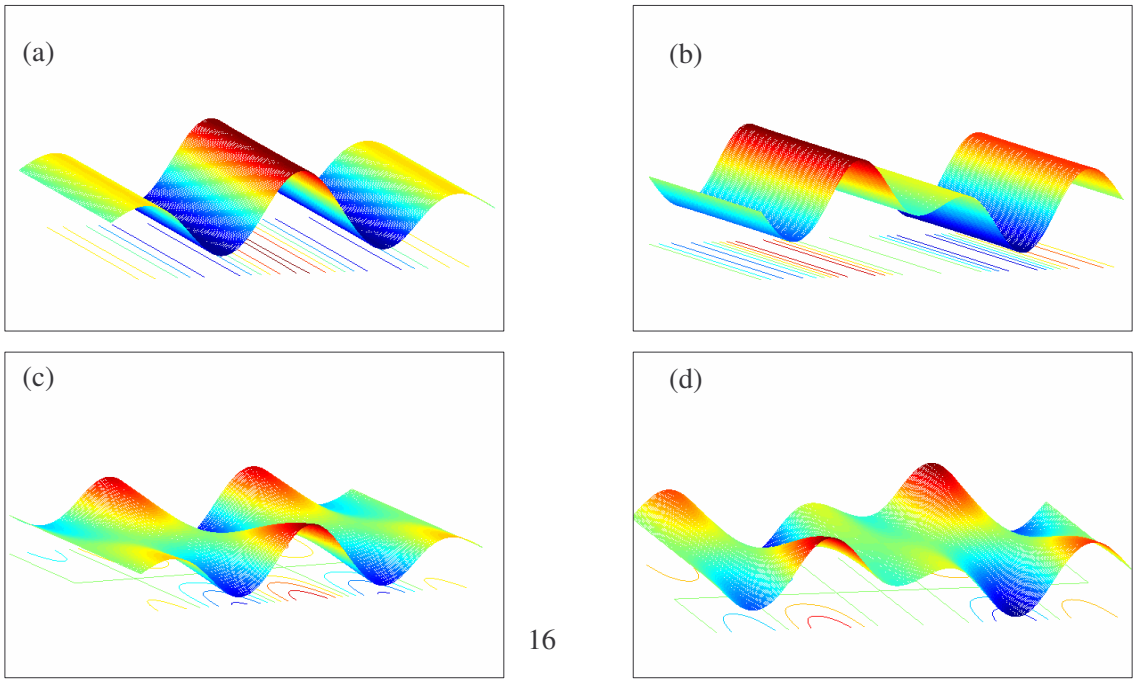

Fig. 6. The first four mode shapes of the five-span bridge deck obtained through the present approach. Modes: (a) 1, f_1 = 3.5936 Hz; (b) 2, f_2 = 4.4942 Hz; (c) 3, f_3 = 4.9186 Hz; (d) 4, f_4 = 5.7455 Hz

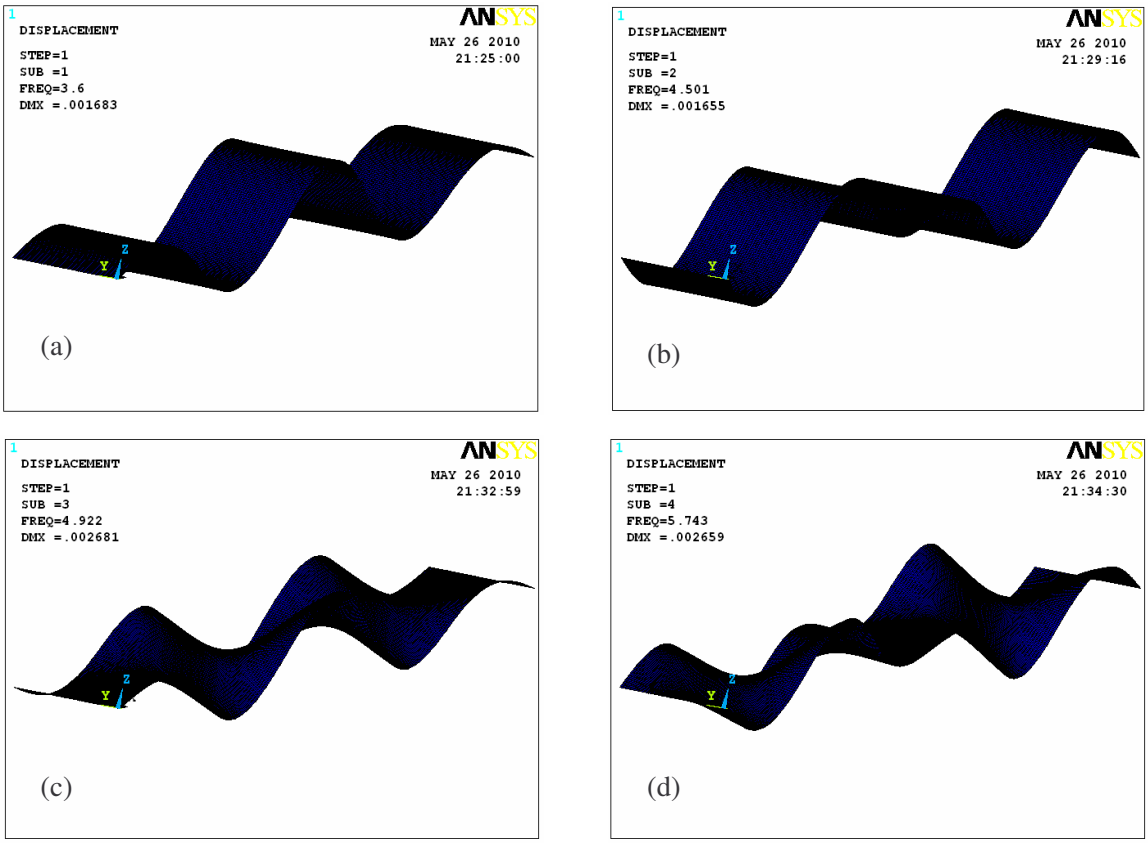

Fig. 7. The first four mode shapes of the five-span bridge deck obtained through ANSYS. Modes: (a) 1, f_1 = 3.5997 Hz; (b) 2, f_2 = 4.5007 Hz; (c) 3, f_3 = 4.9220 Hz; (d) 4, f_4 = 5.7430 Hz

4. Conclusion

In this paper, an extension of a semi-analytical method (Rezaiguia and Laefer, 2009), recently introduced for the calculation of natural frequencies and mode shapes of multi-span continuous, orthotropic roadway bridge deck is presented. This approach is based on the modal superposition method taking into account the effect of intermodal coupling neglected in all previously similar studies. Two numerical examples are reported relative to a four- and five-span bridge deck. Results obtained from the proposed method are in agreement within 2% with those obtained by a finite

element method using ANSYS software. This extension of the semi-analytical method shows its wider applicability for the dynamic analysis of similar bridge decks under moving vehicles, thereby allowing designs a simplified approach with high accuracy levels.

Appendix A

Elements of vector {A} and matrix [F]

The elements in vector {A} are given by

$$\{A\} = \{A_{1i}, A_{2i}, B_{2i}, ..., A_{(R-1)i}, B_{(R-1)i}, A_{Ri}\}^T \tag{A1}$$

The elements in matrix [F] are given by

$$f_{11} = \cos(k_i l_1) - \theta_1 \cosh(k_i l_1), \; f_{12} = \theta_2 - 1, \quad f_{13} = -\Phi_2, \; f_{21} = \sin(k_i l_1), \quad f_{23} = -1 \tag{A2}$$

$$\left.\begin{aligned}
f_{2r-1,\,2(r-1)} &= \cos(k_i l_r) - \theta_r \cosh(k l_r) \\
f_{2r-1,\,2r-1} &= -\sin(k_i l_r) - \sinh(k_i l_r) + \Phi_r \cosh(k_i l_r) \\
f_{2r-1,\,2r} &= \theta_{r+1} - 1 \\
f_{2r-1,\,2r+1} &= -\Phi_{r+1} \\
f_{2r,\,2(r-1)} &= -\sin(k_i l_r) - \theta_r \sinh(k_i l_r) \\
f_{2r,\,2r-1} &= -\cos(k_i l_r) - \cosh(k_i l_r) + \Phi_r \sinh(k_i l_r) \\
f_{2r,\,2r+1} &= 2
\end{aligned}\right\}, \qquad r = 2, 3, ..., R-2 \tag{A3}$$

$$\begin{aligned}
f_{2R-3,\,2(R-2)} &= \theta_{R-1} \cosh(k_i l_{R-1}) - \cos(k_i l_{R-1}) \\
f_{2R-3,\,2R-3} &= \sin(k_i l_{R-1}) + \sinh(k_i l_{R-1}) - \Phi_{R-1} \cosh(k_i l_{R-1}) \\
f_{2R-3,\,2(R-1)} &= \theta_R \cosh(k_i l_R) - \cos(k_i l_R)
\end{aligned}$$

$$\begin{aligned}
f_{2(R-1),\,2(R-2)} &= \sin(k_i l_{R-1}) + \theta_{R-1} \sinh(k_i l_{R-1}) \\
f_{2(R-1),\,2R-3} &= \cos(k_i l_{R-1}) + \cosh(k_i l_{R-1}) - \Phi_{R-1} \sinh(k_i l_{R-1}) \\
f_{2(R-1),\,2(R-1)} &= -2\sin(k_i l_R)
\end{aligned} \tag{A4}$$

where

$$\theta_r = \frac{\sin(k_i l_r)}{\sinh(k_i l_r)}, \qquad \Phi_r = \frac{\cosh(k_i l_r) - \cos(k_i l_r)}{\sinh(k_i l_r)}, \qquad r = 1, 2, ..., R \tag{A5}$$

and the other coefficients f_{ij} equal to zero.

For four- span bridge deck, elements in vector {A} and matrix [F] are given by

$$\{A\} = \{A_{1i}, A_{2i}, B_{2i}, A_{3i}, B_{3i}, A_{4i}\}^T \tag{A7}$$

$$[F] = \begin{bmatrix} \cos(k_i l_1) - \theta_1 \cosh(k_i l_1) & \theta_2 - 1 & -\Phi_2 & 0 & 0 & 0 \\ \sin(k_i l_1) & 0 & -1 & 0 & 0 & 0 \\ 0 & \cos(k_i l_2) - \theta_2 \cosh(k_i l_2) & \begin{array}{c} -\sin(k_i l_2) - \sinh(k_i l_2) \\ +\Phi_2 \cosh(k_i l_2) \end{array} & \theta_3 - 1 & -\Phi_3 & 0 \\ 0 & -\sin(k_i l_2) - \theta_2 \sinh(k_i l_2) & \begin{array}{c} -\cos(k_i l_2) - \cosh(k_i l_2) \\ +\Phi_2 \sinh(k_i l_2) \end{array} & 0 & 2 & 0 \\ 0 & 0 & 0 & \theta_3 \cosh(k_i l_3) - \cos(k_i l_3) & \begin{array}{c} \sin(k_i l_3) + \sinh(k_i l_3) \\ -\Phi_3 \cosh(k_i l_3) \end{array} & \theta_4 \cosh(k_i l_4) - \cos(k_i l_4) \\ 0 & 0 & 0 & +\sin(k_i l_3) + \theta_3 \sinh(k_i l_3) & \begin{array}{c} \cos(k_i l_3) + \cosh(k_i l_3) \\ -\Phi_3 \sinh(k_i l_3) \end{array} & -2\sin(k_i l_4) \end{bmatrix} \tag{A8}$$

For five- span bridge deck, elements in vector {A} and matrix [F] are given by

$$\{A\} = \{A_{1i}, A_{2i}, B_{2i}, A_{3i}, B_{3i}, A_{4i}, B_{4i}, A_{5i}\}^T \tag{A9}$$

$$[F] = \begin{bmatrix}
\cos(k_i l_1) - \theta_1 \cosh(k_i l_1) & \theta_2 - 1 & -\Phi_2 & 0 & 0 & 0 & 0 & 0 \\
\sin(k_i l_1) & 0 & -1 & 0 & 0 & 0 & 0 & 0 \\
0 & \cos(k_i l_2) - \theta_2 \cosh(k_i l_2) & \begin{array}{c} -\sin(k_i l_2) - \sinh(k_i l_2) \\ +\Phi_2 \cosh(k_i l_2) \end{array} & \theta_3 - 1 & -\Phi_3 & 0 & 0 & 0 \\
0 & -\sin(k_i l_2) - \theta_2 \sinh(k_i l_2) & \begin{array}{c} -\cos(k_i l_2) - \cosh(k_i l_2) \\ +\Phi_2 \sinh(k_i l_2) \end{array} & 0 & 2 & 0 & 0 & 0 \\
0 & 0 & 0 & \cos(k_i l_3) - \theta_3 \cosh(k_i l_3) & \begin{array}{c} -\sin(k_i l_3) - \sinh(k_i l_3) \\ +\Phi_3 \cosh(k_i l_3) \end{array} & \theta_4 - 1 & -\Phi_4 & 0 \\
0 & 0 & 0 & -\sin(k_i l_3) - \theta_3 \sinh(k_i l_3) & \begin{array}{c} -\cos(k_i l_3) - \cosh(k_i l_3) \\ +\Phi_3 \sinh(k_i l_3) \end{array} & 0 & 2 & 0 \\
0 & 0 & 0 & 0 & 0 & \theta_4 \cosh(k_i l_4) - \cos(k_i l_4) & \begin{array}{c} \sin(k_i l_4) + \sinh(k_i l_4) \\ -\Phi_4 \cosh(k_i l_4) \end{array} & \theta_5 \cosh(k_i l_5) - \cos(k_i l_5) \\
0 & 0 & 0 & 0 & 0 & \sin(k_i l_4) + \theta_4 \sinh(k_i l_4) & \begin{array}{c} \cos(k_i l_4) + \cosh(k_i l_4) \\ -\Phi_4 \sinh(k_i l_4) \end{array} & -2\sin(k_i l_5)
\end{bmatrix} \tag{A10}$$

References

Bellman R.E. and Casti J. (1971), "Differential quadrature and long-term. integration", *J Math. Anal. and Appl.*, **34**, 235-238.

Cheung, M.S., Cheung, Y.K., and Reddy, D.V. (1971). "Frequency analysis of certain single and continuous span bridges", *In Developments in Bridges Design and Construction*, 188-199.

Davalos J.F., Qiao P., and Shan L. (2006), "Advanced fibre-reinforced polymer (FRP) composites for use in civil engineering", In *Advanced civil infrastructure materials: Science, mechanics and applications*. ed. Wu, H.C., New York: E-Publishing Inc. p. 118-202.

Gorman D.J. and Garibaldi L. (2006), "Accurate analytical type solutions for free vibration frequencies and mode shapes of multi-span bridge decks: the span-by-span approach", *J. Sound Vibr.*, **290**, 321-336.

Hrabok, M.M. and Hrudley, T.M. (1984), "A review and catalogue of plate bending elements", *Comp. and Struct.,* **19**, 479-495.

Lu, C.F., Zhang, Z.C., and Chen, W.Q. (2007), "Free vibration of generally supported rectangular Kirchhoff plates: State-space-based differential quadrature method", *Int'l. J. Num. Methods Eng.,* **70**, 1430-1450.

Ng, S.S.F. and Kaul, V. (1987), "Free vibration analysis of continuous orthotropic Bridge decks", *J. Sound Vibr.*, **119**, 29-38.

Rezaiguia A. (2008), *Vibroacoustic modelling of highway bridges crossing by moving vehicles*. Doctorate Thesis, Annaba University, Algeria.

Rezaiguia A., and Laefer D.F. (2009), "Semi-analytical determination of natural frequencies and mode shapes of multi-span bridge decks", *J. Sound Vibr.*, **328**, 291-300.

Smith, I.M. and William, D. (1970), "The effectiveness of excessive nodal continuities in the finite element analysis of thin rectangular and skew plates in bending", *Int'l. J. Num. Methods Eng.,* **2**, 253-257.

Wu, C.I. and Cheung, Y.K. (1974), "Frequency analysis of rectangular plates continuous in one or two directions", *J. Earthquake Eng. Struc. Dyn.,* **3**, 3-14.

Wu, J.S., Lee, M.L. and Lai, T.S. (1987), "The dynamic analysis of a flat plate under a moving load by the finite element method", *Int'l. J. Num. Methods Eng.* **24**, 743-762.

Zhou, D. and Cheung, Y.K. (1999), "Free vibration of line supported rectangular plates using a set of static beam functions", *J. Sound Vibr*., **223**, 231-245.

Zhu X.Q. and Law S.S. (2001), "Orthogonal functions in moving loads identification on a multispan bridge", *J. Sound Vibr.*, **245**, 329-345.

Zhu, X.Q. and Law, S.S. (2002), "Dynamic loads on continuous multi lane bridge deck from moving vehicles", *J. Sound Vibr*., **251**, 697-716.

Figure/table captions: main text

Fig. 1. Model of the continuous multi-span bridge deck

Fig. 2. Continuous multi-span simply supported beam

Fig. 3. Continuous multi-span multi-girder bridge deck: (a) four span, (b) five span

Fig. 4. The first four mode shapes of the four-span bridge deck obtained through the present approach. Modes: (a) 1, f_1 = 3.7724 Hz; (b) 2, f_2 = 5.0905; (c) 3, f_3 = 5.0927 Hz; (d) 4, f_4 = 6.4501 Hz

Fig. 5. The first four mode shapes of the four-span bridge deck obtained through ANSYS. Modes: (a) 1, f_1 = 3.7736 Hz; (b) 2, f_2 = 5.0891 Hz; (c) 3, f_3 = 5.0978 Hz; (d) 4, f_4 = 6.3290 Hz

Fig. 6. The first four mode shapes of the five-span bridge deck obtained through the present approach. Modes: (a) 1, f_1 = 3.5936 Hz; (b) 2, f_2 = 4.4942 Hz; (c) 3, f_3 = 4.9186 Hz; (d) 4, f_4 = 5.7455 Hz

Fig. 7. The first four mode shapes of the five-span bridge deck obtained through ANSYS. Modes: (a) 1, f_1 = 3.5997 Hz; (b) 2, f_2 = 4.5007 Hz; (c) 3, f_3 = 4.9220 Hz; (d) 4, f_4 = 5.7430 Hz

Table 1. Parametres of four span multi-girder bridge deck

Table 2. Parametres of five span multi-girder bridge deck

Table 3. Mesh density convergence

Table 4. Comparison of natural frequencies of the orthotropic multi-span bridge decks